Phytomedicine 108 (2023) 154489

Contents lists available at ScienceDirect

Phytomedicine

journal homepage: www.elsevier.com/locate/phymed

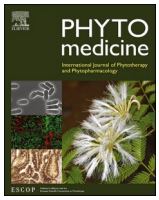

Original Article

Schisandrin B protects against LPS-induced inflammatory lung injury by targeting MyD88

Weiwei Zhu [a,b,c], Wu Luo [d], Jibo Han [a], Qiuyan Zhang [a], Lijun Ji [a,b], Aleksandr V. Samorodov [e], Valentin N. Pavlov [e], Zaishou Zhuang [f], Daona Yang [f], Lina Yin [g], Lijiang Huang [c], Guang Liang [a,f], Joo Young Huh [b,*], Yi Wang [a,b,c,*]

[a] Chemical Biology Research Center, School of Pharmaceutical Sciences, Wenzhou Medical University, Wenzhou, Zhejiang 325035, China
[b] College of Pharmacy, Chonnam National University, Gwangju 61186, Republic of Korea
[c] Affiliated Xiangshan Hospital of Wenzhou Medial University (Xiangshan First People's Hospital Medical and Health Group), Xiangshan, Zhejiang 315799, China
[d] Medical Research Center, The First Affiliated Hospital, Wenzhou Medical University, Wenzhou, Zhejiang 325000, China
[e] Department of Pharmacology, Bashkir State Medical University, Ufa 450005, Russia
[f] The Affiliated Cangnan Hospital, Wenzhou Medical University, Cangnan, Zhejiang 325800, China
[g] School of Pharmaceutical Sciences, Hangzhou Medical College, Hangzhou, Zhejiang 311399, China

ARTICLE INFO

Keywords:
Schisandrin B
MyD88
TLR4
Inflammation
Acute lung injury
NF-κB

ABSTRACT

Background: Acute lung injury (ALI) is a challenging clinical syndrome that manifests as an acute inflammatory response. Schisandrin B (Sch B), a bioactive lignan from *Schisandra* genus plants, has been shown to suppress inflammatory responses and oxidative stress. However, the underlying molecular mechanisms have remained elusive.

Hypothesis/purpose: This study performed an in-depth investigation of the anti-inflammatory mechanism of Sch B in macrophages and in an animal model of ALI.

Methods: qPCR array was used to probe the differential effects and potential target of Sch B. ALI was induced by intratracheal administration of LPS in experimental mice with or without Sch B treatment.

Results: Our studies show that Sch B differentially modulates inflammatory factor induction by LPS in macrophages by directly binding myeloid differentiation response factor-88 (MyD88), an essential adaptor protein in the toll-like receptor-4 (TLR4) pathway. Sch B spares non-MyD88-pathways downstream of TLR4. Such inhibition suppressed key signaling mediators such as TAK1, MAPKs, and NF-κB, and pro-inflammatory factor induction. Pull down assay using biotinylated-Sch B validate the direct interaction between Sch B and MyD88 in macrophages. Treatment of mice with Sch B prior to LPS challenge reduced inflammatory cell infiltration in lungs, induction of MyD88-pathway signaling proteins, and prevented inflammatory cytokine induction.

Conclusion: In summary, our studies have identified MyD88 as a direct target of Sch B for its anti-inflammatory activity, and suggest that Sch B may have therapeutic value for acute lung injury and other MyD88-dependent inflammatory diseases.

Introduction

Acute respiratory distress syndrome (ARDS), a complex disease that starts with acute lung injury (ALI) in response to various direct or indirect insults, has high morbidity and mortality rate (Matthay et al., 2019). Despite efforts to understand the pathophysiology, current

Abbreviations: ALI, acute lung injury; BALF, bronchoalveolar lavage fluid; CCL2, chemokine (C—C motif) ligand 2; CCL5, chemokine (C—C motif) ligand 5; ERK, extracellular signal-regulated kinase; IFN-β, interferon β; IFN-γ, interferon γ; IκB-α, inhibitor of κBα; IL-1β, interleukin 1β; IL-6, interleukin 6; IL-12, interleukin 12; IRF3, interferon regulatory factor 3; JNK, c-Jun N-terminal kinase; MAPK, mitogen-activated protein kinase; MD2, myeloid differentiation factor 2; MyD88, myeloid differentiation primary response factor 88; Sch B, schisandrin B; TAK1, transforming growth factor beta-activated kinase 1; TBK1, TANK binding kinase 1; TLR4, toll-like receptor 4; TNF-α, tumor necrosis factor α; TRIF, TIR-domain-containing adapter-inducing interferon-β.

* Corresponding author at: Chemical Biology Research Center, School of Pharmaceutical Sciences, Wenzhou Medical University, Wenzhou, Zhejiang, 325035, China.

E-mail addresses: jooyhuh@chonnam.ac.kr (J.Y. Huh), yi.wang1122@wmu.edu.cn (Y. Wang).

https://doi.org/10.1016/j.phymed.2022.154489
Received 16 November 2021; Received in revised form 25 September 2022; Accepted 3 October 2022
Available online 12 October 2022

treatments for ALI/ARDS are primarily supportive and include mechanical ventilation and corticosteroid administration (Banavasi et al., 2021). However, the unchanged mortality in restrictive fluid supportive management and ventilator-associated side effects have been widely reported (Liu et al., 2022b). Hence, a safe and effective therapeutic approach for ALI/ARDS is urgently needed.

The innate immune response plays a profound role in the pathophysiology of ARDS and ALI. This response includes lung injury mediated by macrophages, neutrophils, and lymphocytes (Wong et al., 2019). Following early injury in the alveolar epithelium, inflammatory cells migrate into the lung tissue (Wong et al., 2019). Subsequently, inflammatory mediators are released into the systemic circulation, which potentiate lung injury. Infiltrating inflammatory cells release a host of cytokines and proinflammatory factors (Kany et al., 2019), including tumor necrosis factor-alpha (TNF-α), interleukins 1 (IL-1), and IL-6. Therefore, the anti-inflammatory strategy could be a valuable direction in the treatment of ALI/ARDS.

Experimentally, ALI/ARDS is commonly generated by administering bleomycin, acids, or lipopolysaccharide (LPS) in rodents (D'Alessio, 2018; Rao et al., 2021). On a cellular basis, LPS stimulation occurs through a series of interactions with proteins including myeloid differentiation factor-2 (MD2) and toll-like receptor-4 (TLR4) (Fitzgerald and Kagan, 2020). Once LPS is recognized by TLR4, intracellular adapter proteins, such as myeloid differentiation primary response factor-88 (MyD88) and TIR-domain-containing adapter-inducing interferon-β (TRIF) are recruited. Signaling through the MyD88 pathway is well-characterized and involves cascading activation of transforming growth factor-β-activated kinase 1 (TAK1), mitogen-activated protein kinase (MAPK), and nuclear factor-κB (NF-κB) (Ciesielska et al., 2021). The end result is the induction of pro-inflammatory cytokines including TNF-α and IL-6. In addition, the TRIF pathway induces type I interferons and interferon-inducible genes *via* TANK binding protein 1 (TBK1) and interferon regulatory factor-3 (IRF3). In addition to providing insight into ALI/ARDS, LPS-challenge models also offer an excellent platform for the discovery of novel anti-inflammatory targets and pharmacodynamic efficacy of drugs.

Various herbal plants have been reported to show a plethora of desired pharmacological properties against acute and chronic diseases (Atanasov et al., 2021; Rahman et al., 2022) . One such promising plant is *Schisandra chinensis*, which is native to northeastern China, Japan, Korea, and other places. It has been used as a herbal supplement in both traditional Chinese medicine and Western phytotherapy (Nowak et al., 2019; Rybnikar et al., 2019). Schisandrin B (Sch B, Fig. 1A) is one of the dominant lignans in *Schisandra chinensis* (Gao et al., 2019). Sch B has been shown to activate the antioxidant defense system in different animal models (Kopustinskiene and Bernatoniene, 2021; Wu et al., 2019). However, recent studies have also shown an anti-inflammatory activity of Sch B (Nasser et al., 2020). For example, Sch B was recently shown to suppress NF-κB activation induced by ovalbumin (OVA) in a mouse model of allergic asthma (Chen et al., 2021). In an ischemic cardiac injury model, Sch B prevents the induction of IL-1β, TNF-α, IL-6, and IL-8 (Zhao et al., 2021). Our group has also found that Sch B inhibits NF-κB activation to alleviate angiotensin II-induced vascular injury (You et al., 2019). Based on these features, we believed that Sch B is a potential candidate in the treatment of ALI/ARDS. However, the direct molecule targets of Sch B supporting its biological activities are still unknown.

In the present study, we explored the effects of Sch B in LPS-induced inflammation both *in vitro* and *in vivo*. Also, we investigated the potential mechanisms by which Sch B provides anti-inflammatory activity and affects ALI. These studies may provide a novel targeted drug for the treatment of acute inflammatory diseases.

Materials and methods

Reagents

Schisandrin B (Sch B, purity > 98%) was purchased from Selleck Chemicals (Houston, TX, USA). Biotinylated-Sch B (Bio-Sch B) was purchased from Fanbo Biochemicals (Beijing, China). Biotin (Bio; Cat# B4501) and lipopolysaccharide (LPS from E. coli; Cat# L2630) were purchased from Sigma-Aldrich (St. Louis, MO, USA). Pam3CSK4 was purchased from Glpbio (Montclair, CA, USA). Antibodies against GAPDH (Cat# 5174), TAK1 (Cat# 5206), phosphorylated (p-) TAK1 (Cat# 9339), extracellular signal-regulated kinase 1/2 (ERK1/2; Cat# 9102), p-ERK1/2 (Cat# 9101), c-Jun N-terminal kinase (JNK; Cat# 9252), p-JNK (Cat# 9251), p38 (Cat# 8690), p-p38 (Cat# 9211), TBK1 (Cat# 3013), p-TBK1 (Cat# 5483), IRF3 (Cat# 11,904), p-IRF3 (Cat# 37,829), MyD88 (Cat# 4283), and TRIF (Cat# 4596) were purchased from Cell Signaling Technology (Danvers, MA, USA). Antibodies against TLR4 (Cat# sc-293,072) and inhibitor of κBα (IκB-α; Cat# sc-1643) were purchased from Santa Cruz Biotechnology (Santa Cruz, CA, USA). Antibodies against MD2 (Cat# ab24182), TLR2 (Cat# ab209217), TNF-α (Cat# ab183218), IL-6 (Cat# ab233706), and macrophage marker F4/80 (Cat# ab6640) were purchased from Abcam (Cambridge, UK). FLAG- (Cat# SAB4200071) and HA- (Cat# H9658) antibodies were purchased from Sigma-Aldrich. Fluorophore-labeled antibodies including PerCP-anti-CD45 (Cat# 103,130), PE-anti-F4/80 (Cat# 123,110), APC-anti-CD11b (Cat# 101,212), and FITC-anti-Ly6C (Cat# 128,006) were purchased from BioLegend (San Diego, CA, USA).

Cell culture

Mouse macrophage cell line RAW264.7 was purchased from Shanghai Institute of Biochemistry and Cell Biology (Shanghai, China) and cultured in Dulbecco's Modified Eagle Medium (DMEM; Gibco, Thermo Fisher) with high glucose and 10% fetal bovine serum (FBS; Gibco), and 1% penicillin/streptomycin (Invitrogen; Waltham, MA, USA). Mouse primary peritoneal macrophages (MPMs) were prepared from C57BL/6 mice as described previously (Chen et al., 2019). Briefly, mice were stimulated by intraperitoneal injection of 6% thioglycolate solution (0.3 g beef extract, 1 g tryptone and 0.5 g sodium chloride dissolved in 100 ml ddH_2O and filtrated through a 0.22 μm filter; 2 ml used *per* mouse) and kept in a pathogen-free condition for 3 days before cell isolation. Total MPMs were harvested by washing the peritoneal cavity with 8 ml RPMI-1640 medium (Gibco). The cell collection medium was centrifuged and resuspended in RPMI-1640 medium with 10% FBS and 1% penicillin/streptomycin. Primary cultures were prepared at a density of 700,000 cells *per* 35 mm diameter well and used 24 h after plating. Non-adherent cells were removed by washing with fresh medium 4 h after seeding.

Animal modeling of ALI

All animals received humane care according to the National Institutes of Health (NIH; Bethesda, MD, USA) guidelines. All animal care and experimental procedures were approved by the Animal Policy and Welfare Committee in Wenzhou Medical University (Approved number: wydw2020–0012). Six-week-old male C57BL/6 mice (totally $n = 30$) were obtained from the Animal centre of Wenzhou Medical University (Wenzhou, Zhejiang, China). All animals were housed in a pathogen-free room under 22 ± 2 °C, 50–60% humidity, 12:12 h light-dark cycle, and fed with a standard rodent diet and water. The animals were acclimatized to the laboratory for 2 weeks before initiating the studies. All animal experiments were performed and analyzed by blinded experimenters. Randomization was used when dividing the groups. Each mouse was assigned a temporary random number within the weight range and was then given its permanent numerical designation in the cages. For each group, a cage was selected randomly from the pool of all

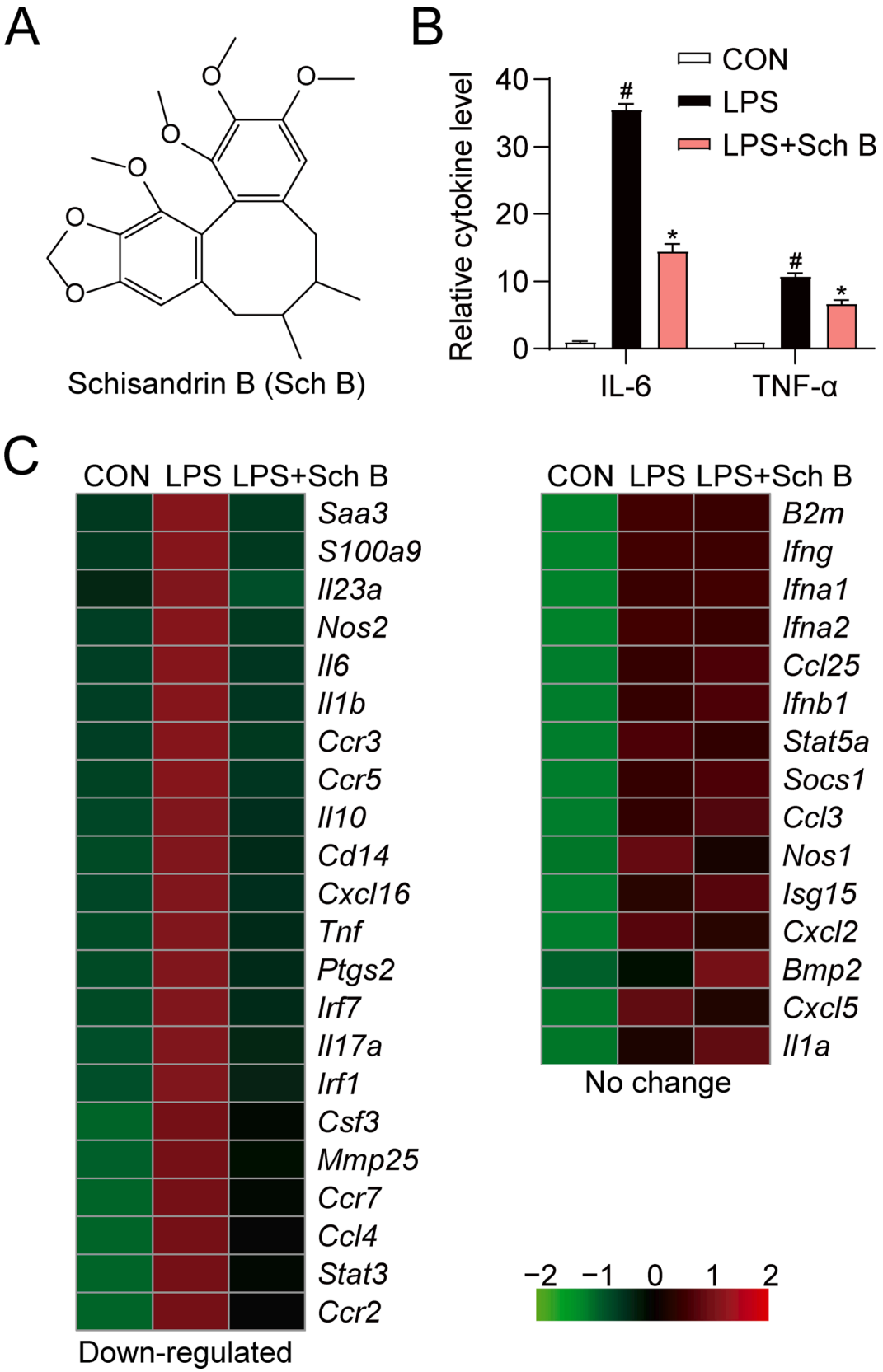

Fig. 1. Identification of Schisandrin B-regulated inflammatory factors. (A) Chemical structure of Schisandrin B (Sch B). (B) RAW264.7 cells were pretreated with Sch B at 10 μM for 30 min and then exposed to LPS at 0.5 μg/ml for 24 h. DMSO was used as vehicle control. IL-6 and TNF-α levels in the culture medium were measured. (C) RAW264.7 cells were pretreated with Sch B at 10 μM for 30 min and then treated with LPS at 0.5 μg/ml for 6 h. mRNA levels of inflammatory factors were determined. Data was normalized to *Hprt1*. Figure showing heatmap of down-regulated genes ($p<0.5$ change compared to LPS) and genes showing no significant change (levels 0.67 – 1.5× LPS). Data are shown in Mean ± SEM; n=3 *per* group; #$p<0.05$ compared to CON; *$p<0.05$ compared to LPS.

cages.

Mice were randomly divided into five groups ($n = 6$ *per* group): (1) mice treated with vehicle control (CON); (2) mice treated with 20 $mg{\cdot}kg^{-1}$ Sch B (Sch B 20) (3) LPS-challenged mice (LPS); (4) LPS-challenged mice treated with 10 $mg{\cdot}kg^{-1}$ Sch B (LPS+Sch B 10); (5) LPS-challenged mice treated with 20 $mg{\cdot}kg^{-1}$ Sch B (LPS+Sch B 20). Sch B was dissolved in 0.5% sodium carboxymethyl cellulose (CMC—Na) and administered orally at a volume of 10 $\mu{\cdot}g^{-1}$ body weight every 12 h for 36 h, prior to the LPS challenge. CON and LPS groups received the same volume of 0.5% CMC—Na only. ALI was induced essentially as described previously. Briefly, following Sch B pre-treatment, mice were anesthetized with 2% sodium pentobarbital (80 $mg{\cdot}kg^{-1}$, i.p., Sigma-Aldrich). Heart rate, body temperature, and toe pinch were monitored to detect the depth of anesthesia. Mice were then challenged by intratracheal injection of LPS (5 $mg{\cdot}kg^{-1}$; dissolved in 0.9% saline) or 0.9% saline alone. At 6 h post-LPS challenge, mice were sacrificed and bronchoalveolar lavage fluid (BALF) was collected through the tracheal cannula. Blood and lung tissue samples were collected for subsequent analyses.

Collected BALF samples were centrifuged at 3000 rpm for 5 min. The supernatant was used for determining total protein levels and levels of cytokines using ELISA. Cell pellets were resuspended in 100 µl 0.9% saline, and the total cell counts were determined with a hemocytometer. Neutrophil count was acquired by counting 200 cells on a smear prepared by Wright–Giemsa staining (Nanjing Jiancheng Bioengineering Institute; Nanjing, Jiangsu, China). Lung wet/dry weights were determined as an index of pulmonary edema. The right middle lobes were collected, and wet weights were recorded. Tissues were heated in a thermostatically controlled oven at 65 °C for 72 h, and dry weights were measured.

Lung histology and immunostaining

Lung tissues were fixed in 4% paraformaldehyde, embedded in paraffin, and sectioned at 5 µm thickness. For routine histology, sections were stained with hematoxylin and eosin (H&E; Sigma). Lung injury scores (0–1) were determined by using criterion (Paris et al., 2020) presented in Supplementary Table S1. Final injury scores were calculated as: Score = [(20 × A) + (14 × B) + (7 × C) + (7 × D) + (2 × E)]/(number of fields × 100).

Immunostaining was performed on deparaffinized and hydrated lung sections. Antigen retrieval was performed by heating sections in sodium citrate buffer (pH 6.0). Sections were blocked in 1% bovine serum albumin (BSA; Sigma-Aldrich) in PBS for 30 min and incubated with primary antibody (1:100) overnight at 4 °C. Horseradish peroxidase (HRP)-labeled secondary antibodies were applied for 1 h at 37 °C. Immunoreactivity was detected by diaminobenzidine (DAB). Sections were counterstained with hematoxylin. Images were captured using a brightfield microscope. Image J analysis software version 1.53i (NIH; Bethesda, MD, USA) was used to calculate immunoreactivity.

Myeloperoxidase activity assay

Neutrophil tissue infiltration was evaluated by myeloperoxidase (MPO) activity in lung tissue samples by using the MPO Detection Kit (Nanjing Jiancheng Bioengineering Institute). Lung tissues were homogenized in 1 ml of 50 mM potassium PBS (pH 6.0) containing 0.5% hexadecyltrimethylammonium hydroxide and centrifuged at 15,000 g at 4 °C for 20 min. Ten µl of the supernatant was transferred into PBS (pH 6.0) containing 0.17 mg/ml 3,3′-dimethoxybenzidine and 0.0005% H_2O_2. MPO activity in the supernatant was determined by measuring absorbance at 460 nm. Total protein levels were measured using Pierce BCA Protein assay kit (23,225; Thermo Fisher; Carlsbad, CA, USA). Data was presented as U/g tissue.

Flow cytometric determination of infiltrating cells

Cell pellets prepared from BALF were resuspended in 100 µl FACS buffer (PBS with 2% FBS and 1 mM EDTA). Cells were stained with PerCP-anti-CD45, PE-anti-F4/80, APC-anti-CD11b, and FITC-anti-Ly6C for 30 min on ice. Cells were then washed three times with FACS buffer and detected using BD Accuri™ C6 Cytometer (BD Biosciences; Franklin Lakes, NJ, USA). Total viable cells were first gated for CD45-positive immune cells and analyzed for F4/80, CD11b, and Ly6C. Monocytes were presented as $CD11b^{+}$-$Ly6C^{+}$ and macrophages as $CD11b^{+}$-$F4/80^{+}$.

ELISA assay for cytokines

Cytokines were detected in cell culture media and mouse serum and BALF samples. Total proteins were determined for normalization. Commercially available mouse TNF-α and IL-6 ELISA kits (eBioscience; San Diego, CA, USA) were used for these studies. Absorbance was measured at 450 nm using SpectraMax M5 Multi-Mode Microplate Reader (Molecular Devices, San Jose, CA).

Real-time qPCR assay

Total RNA from cells and mouse tissues was extracted using Trizol Reagent (MRC; Cincinnati, OH, USA). RNA was reverse-transcribed using PrimeScript™ RT reagent Kit (Takara; Tokyo, Japan). Real-time qPCR was performed using TB Green® Premix Ex Taq™ II (Takara) on CFX96 Touch Real-Time PCR Detection System (Bio-Rad; Hercules, CA, USA). Target gene sequences are shown in Supplementary Table S2. Target transcript levels were normalized to *Actb*. For some studies, we utilized a pre-coated inflammatory factor qPCR Array (CT Bioscience; Changzhou, Jiangsu, China). Data from pre-loaded arrays was normalized to *Hprt1*.

Schisandrin B-MyD88 binding assay

We examined the binding of Sch B to MyD88 using the Pierce biotinylated protein interaction pull-down kit (21,115; Thermo Fisher). A 100 µl solution of 20 mM biotinylated-Sch B was added to 50 µl streptavidin-agarose beads and incubated at 4 °C for 30 min. Biotin alone was used as a control. Lysates prepared from RAW264.7 cells were added. The mixture was incubated at 4 °C for 24 h with gentle rocking. Samples were then spun and washed 3 times. Elution Buffer was added onto each spin column. The eluent was boiled with 5× loading buffer, and the samples were loaded on a 10% polyacrylamide gel for Western Blot analysis. Total lysates were used as input control.

MyD88 silencing and expression

MyD88 was silenced in RAW264.7 cells by siRNA. Mouse MyD88 siRNA sequences (Forward: 5'-GCCAGAAAUACUUAGGUAATT-3'; Reverse: 5'-UUACCUAAGUAUUUCUGGCTT-3') were purchased from GenePharma (Shanghai, China). Negative control transfections included scrambled siRNA sequences. To investigate the dimerization of MyD88, Flag- and HA-tagged MyD88 was expressed by co-transfecting cells with pcDNA3.1-MyD88-Flag and pcDNA3.1-MyD88-HA plasmids (Shanghai GeneChem Co, Shanghai, China). Transfections were carried out using LipofectAMINE™ 2000 (Invitrogen).

Western blot and immunoprecipitation

Proteins were isolated using RIPA lysis and extraction buffer (89,900; Thermo Fisher) and concentrations were measured using Pierce BCA Protein assay kit. Protein lysates were separated by sodium dodecyl sulfate-polyacrylamide gel electrophoresis and transferred to polyvinylidene fluoride membranes. The membranes were blocked with

skimmed milk for 1 h at room temperature and incubated with primary antibodies at 4℃ overnight. Secondary antibodies were applied for 1 h at room temperature. Immunoreactivity was visualized using enhanced chemiluminescence reagents (Bio-Rad). Protein-protein interaction was evaluated by co-immunoprecipitation. Protein lysates were incubated with specific precipitating antibodies at 4 ℃ overnight, precipitated with protein A/G agarose beads (Santa Cruz), and used for detection of interacting proteins by immunoblotting. Image J analysis software version 1.38e was used for densitometric quantification of blots. Densitometric quantification data was normalized to total proteins or loading controls.

Statistical analysis

All data are expressed as Mean ± SEM. GraphPad Prism 8.0 software (San Diego, CA, USA) was used for statistical analysis. *Student's t*-test was applied when comparing two groups of data. One-way ANOVA followed by Dunnett's post hoc test was used when comparing more than two groups of data. *P* value < 0.05 was considered significant in statistics. Post-tests were run if F achieved $p < 0.05$ and there was no significant variance inhomogeneity.

Results

Sch B suppresses inflammatory factor induction in macrophages through regulating MyD88 pathway

Our first objective was to confirm that Sch B provides anti-inflammatory activity in macrophages. We pretreated RAW264.7 cells with 10 μM Sch B and then exposed the cells to LPS. Levels of IL-6 and TNF-α were induced by LPS but Sch B pretreatment was associated with significantly reduced cytokine induction in macrophages (Fig. 1B). To examine whether such anti-inflammatory activity was restricted to IL-6 and TNF-α, we profiled multiple inflammatory factors using qPCR assay. We show that Sch B had a differential effect on inflammatory genes in macrophages. A large number of genes were downregulated (Fig. 1C)

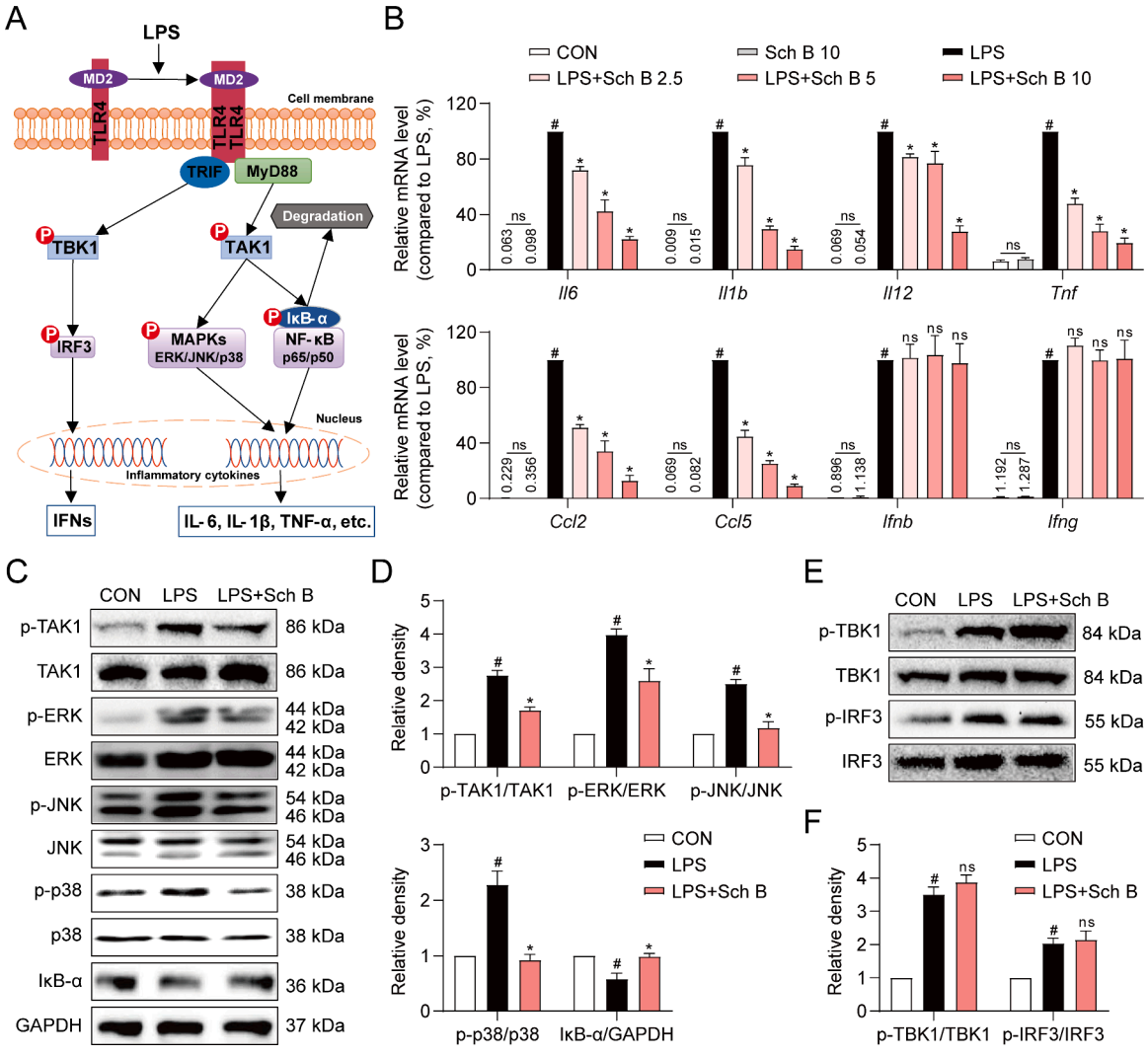

Fig. 2. Sch B suppresses MyD88-dependent pathway but not the TRIF-dependent pathway in macrophages. (A) Schematic showing the toll-like receptor-4 (TLR4) signaling pathway and the downstream MyD88-dependent and -independent branches. (B) RAW264.7 cells were pretreated with Sch B (2.5, 5, 10 μM) for 30 min and then treated with 0.5 μg/ml LPS for 6 h. mRNA levels of key inflammatory factors downstream of MyD88-dependent and -independent pathways were measured. Data normalized to *Actb*. (C, D) RAW264.7 cells were pretreated with 10 μM Sch B for 30 min and then exposed to 0.5 μg/ml LPS for 1 h. Activation of the MyD88-dependent pathway was assessed by probing for IκBα and phosphorylated TAK1 and MAPK (ERK1/2, JNK, and p38) proteins. GAPDH was used as loading control. Representative immunoblots are shown in C and densitometric quantification in D. (E, F) Activation of the TRIF-dependent pathway was assessed in RAW264.7 cells. Cells were treated as in Panel C. Level of phosphorylated TBK1 and IRF3 were determined. Representative immunoblots are shown in E and densitometric quantification in F. Data are shown in Mean ± SEM; n=3 *per* group; ns = not significant; #p<0.05 compared to CON; *p<0.05 compared to LPS.

and these included classical inflammatory factors such as *Il1b, Il6*, and *Tnf*. However, we also found some genes that were not altered (Fig. 1C) or even upregulated after Sch B pretreatment (Supplementary Fig. S1). As shown in the right image in Fig. 1C, interestingly, all genes in the interferon family, which were up-regulated by LPS challenge, failed to be affected by Sch B. The changing profile of Sch B on inflammatory genes promoted us to analyze the known inflammatory signaling pathway and to deduce possible anti-inflammatory mechanism of Sch B.

We know that LPS mediates inflammatory responses through TLR4. Upon LPS recognition, TLR4 undergoes oligomerization and recruits downstream adaptors (MyD88 and TRIF) (Ciesielska et al., 2021). Primarily based on studies using macrophages, a MyD88-dependent pathway was shown to regulate pro-inflammatory cytokines and a MyD88-independent pathway (TRIF) for the induction of type I interferons and interferon-inducible genes (Fig. 2A). To build on our qPCR profiling data, we assessed the levels of select inflammatory and

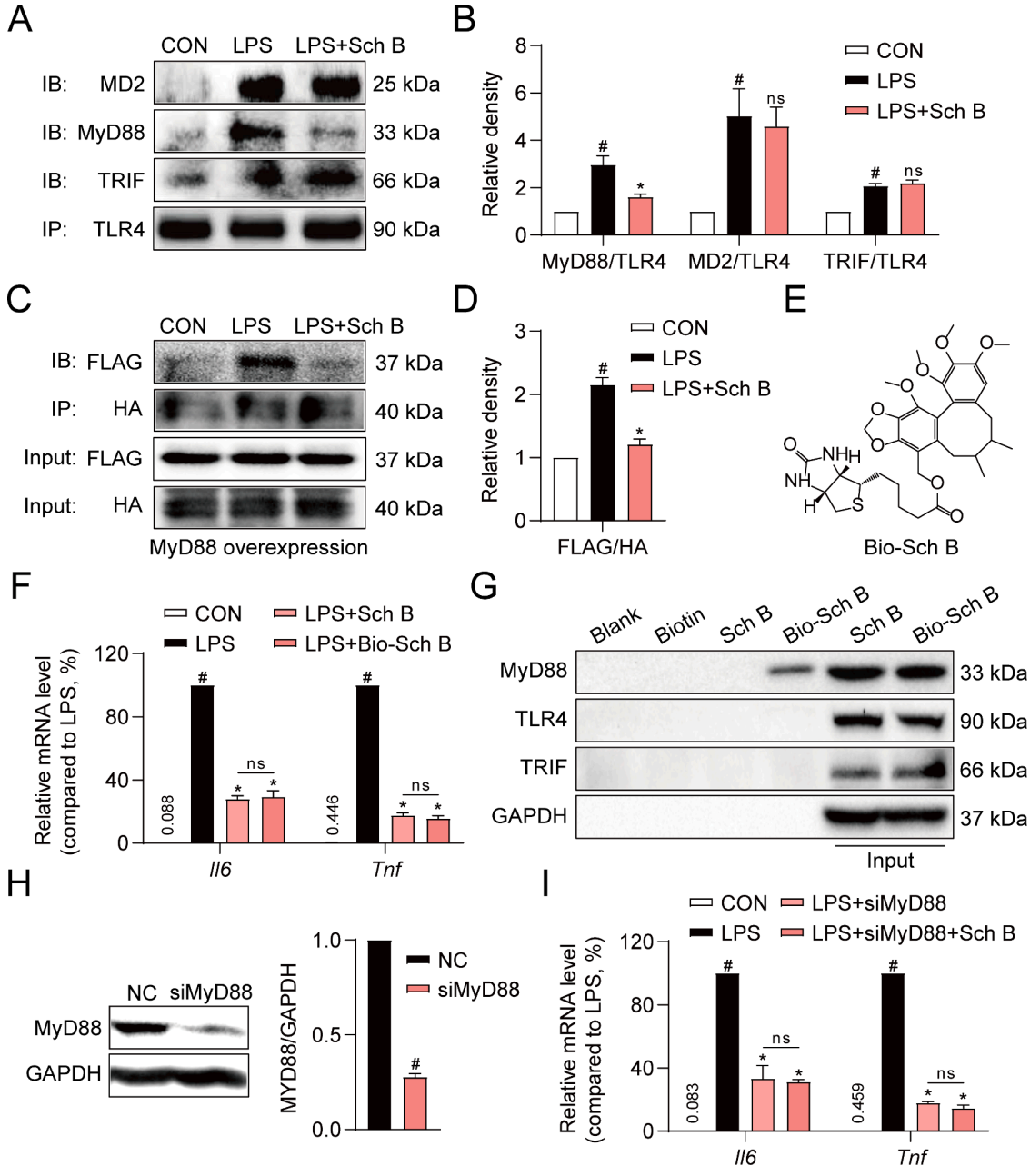

Fig. 3. Sch B binds to MyD88 protein. (A, B) RAW264.7 cells were pretreated with 10 μM Sch B for 30 min and then exposed to 0.5 μg/ml LPS for 1 h. The interaction between TLR4 (IP) and MyD88, MD2, and TRIF (IB) was assessed by co-immunoprecipitation. Representative immunoblots shown in A and densitometric quantification is shown in B. (C, D) RAW264.7 cells were co-transfected with MyD88-FLAG and MyD88-HA plasmids. Cells were then pretreated with 10 μM Sch B for 30 min and exposed to 0.5 μg/ml LPS for 1 h. MyD88 dimerization was measured. Representative immunoblots shown in C and densitometric quantification is shown in D. (E) Chemical structure of biotinylated-Sch B (Bio-Sch B). (F) RAW264.7 cells were pretreated with 10 μM Sch B or Bio-Sch B for 30 min. Cells were then exposed to 0.5 μg/ml LPS for 6 h. mRNA levels of *Il6* and *Tnf* were measured. Data normalized to *Actb*. (G) RAW264.7 lysates were mixed with Bio-Sch B. Interacting proteins were pulled down using streptavidin-agarose beads. Free biotin and unbiotinylated Sch B were used as control. (H) RAW264.7 cells were transfected with MyD88 siRNA. Control cells were transfected with negative control (scrambled; NC) siRNA. Western blot was used to determine knockdown efficiency. Densitometric quantification is shown on right. (I) Cytokine levels following LPS exposure were measured in RAW264.7 cells that had been transfected with siMyD88. In one group, transfected cells were pretreated with 10 μM Sch B for 30 min. Cells, pretreated or untreated, were exposed to 0.5 μg/ml LPS for 6h. mRNA levels of *Il6* and *Tnfa* were measured. Data normalized to *Actb*. Data are shown in Mean ± SEM; n=3 *per* group; ns = not significant; # p <0.05 compared to CON; * p <0.05 compared to LPS.

interferon response genes in macrophages. Our results show that Sch B dose-dependently suppressed the LPS-induced expression of *Il6, Il1b, Il12, Tnf, Ccl2* and *Ccl5* (Fig. 2B). However, *Ifnb* and *Ifng* were not suppressed by Sch B pretreatment. Similar results were obtained in primary mouse macrophages (Supplementary Fig. S2). These results suggest that Sch B suppresses the MyD88-dependent pathway rather than LPS-induced TRIF pathway. Indeed, levels of inhibitor of κBα (IκBα; negative regulator of NFκB) were increased by Sch B pretreatment, whereas levels of phosphorylated TAK1 and MAPKs (ERK, JNK, and p38) were reduced (Fig. 2C, D). Furthermore, levels of LPS-induced phosphorylated TBK1 and IRF3 in the TRIF signaling pathway were not altered by Sch B pre-treatment (Fig. 2E, F).

Sch B suppresses MyD88-pathway by directly binding to MyD88 and reducing its interaction with TLRs

It is interesting that Sch B inhibits MyD88 signal, but not TRIF signal. We next assessed the effect of Sch B on the interaction of TLR4 with MyD88 and TRIF in macrophages exposed to LPS. Based on our studies above, we anticipated that Sch B would only interfere with TLR4-MyD88 interaction. We immunoprecipitated TLR4 and found reduced levels of associated MyD88 proteins when cells were treated with Sch B prior to LPS challenge (Fig. 3A, B). Neither MD2-TLR4 interaction nor TLR4-TRIF interaction in LPS-stimulated macrophages was altered by Sch B pretreatment. These data indicate that Sch B may directly target the MyD88 protein or the TLR4 protein domain involved in TLR4-MyD88 interaction. We then co-transfected RAW264.7 cells with Flag- and HA-tagged MyD88 to determine whether Sch B has an effect on MyD88 oligomerization, which is critical for signaling (Moncrieffe et al., 2020). Our results show that Sch B almost completely normalized LPS-induced MyD88 oligomerization (Fig. 3C, D). These results suggested us to determine whether Sch B directly binds to MyD88 and prevents its homo- and hetero-oligomerization. To validate this hypothesis, we utilized biotinylated-Sch B (Bio-Sch B; Fig. 3E) to pull down associating proteins. Such biotinylation of Sch B does not alter its biological activity as assessed by equivalent *Il6* and *Tnf* suppressive activity as with Sch B (Fig. 3F). Addition of RAW264.7 cell lysates to Bio-Sch B showed interaction with MyD88 but not TLR4 and TRIF (Fig. 3G), validating the direct and specific interaction between Sch B and MyD88 protein. We further confirmed the role of MyD88 in Sch B-mediated anti-inflammatory activity by knocking down *Myd88* expression in RAW264.7 cells (Fig. 3H). Knocking down *Myd88* to approximately 80% of control eliminated innately protective effect of Sch B in LPS-induced inflammation (Fig. 3I). These data suggest that Sch B binds to MyD88 and suppresses LPS-TLR4 inflammatory response.

In addition to TLR4, MyD88 is an adaptor protein of other TLRs such as TLR2 (Dutta et al., 2021). We also examined if Sch B affects other TLRs *via* targeting MyD88. We immunoprecipitated TLR2 and showed reduced levels of associated MyD88 protein when cells were treated with Sch B prior to Pam3CSK4 (Pam, a TLR2 agonist) challenge (Supplementary Fig. S3A, B). As expected, Pam3CSK4-induced inflammatory cytokines, including *Il6* and *Tnf*, were all inhibited by Sch B pretreatment (Supplementary Fig. S3C). These results match the finding that Sch B targets MyD88.

Sch B protects against LPS-induced inflammatory lung injury in mice

TLR4-MyD88 signaling pathway has been shown to play an important role in LPS-induced ALI. Our next objective was to validate our *in vitro* data in a mouse model of inflammatory ALI. Mice were treated with Sch B at 10 or 20 mg/kg and then challenged with LPS for 6 h. LPS increased the protein content in bronchoalveolar lavage fluid (BALF), a common surrogate for increased pulmonary vascular permeability and injury (Fig. 4A). In addition, wet:dry lung weight ratio and histopathological injury scores were significantly higher in LPS-challenged mice (Fig. 4B, D). Tissues showed pulmonary edema, hemorrhage, leukocytic infiltration, and increased thickness of the alveolar wall. Treatment with either 10 or 20 mg/kg Sch B prior to LPS challenge reduced lung injury in mice as assessed by BALF protein content, lung wet:dry weight, and injury scores. We proceeded with assessment of inflammatory factors in the mice. Sch B reduced the levels of LPS-induced IL-6 and TNF-α in BALF as well as in the serum (Fig. 5A-D). Immunohistochemical staining of lung tissues also showed increased IL-6 and TNF-α immunoreactivity upon LPS challenge (Fig. 5E-H). As expected, lungs from Sch B-treated mice showed significantly reduced IL-6 and TNF-α immunoreactivity. These results show that Sch B provides protection against LPS-induced lung inflammation and reduces lung injury.

Protection by Sch B against LPS-induced lung injury is mediated through reduced infiltration and MyD88 inhibition

To investigate the mechanisms of reduced LPS-induced lung injury by Sch B, we analyzed BALF samples for inflammatory cells. Total cell counts, as well as neutrophils, were increased in BALF samples obtained from mice challenged with LPS (Fig. 6A, B). Sch B treatment significantly reduced these increases. Furthermore, myeloperoxidase (MPO), a

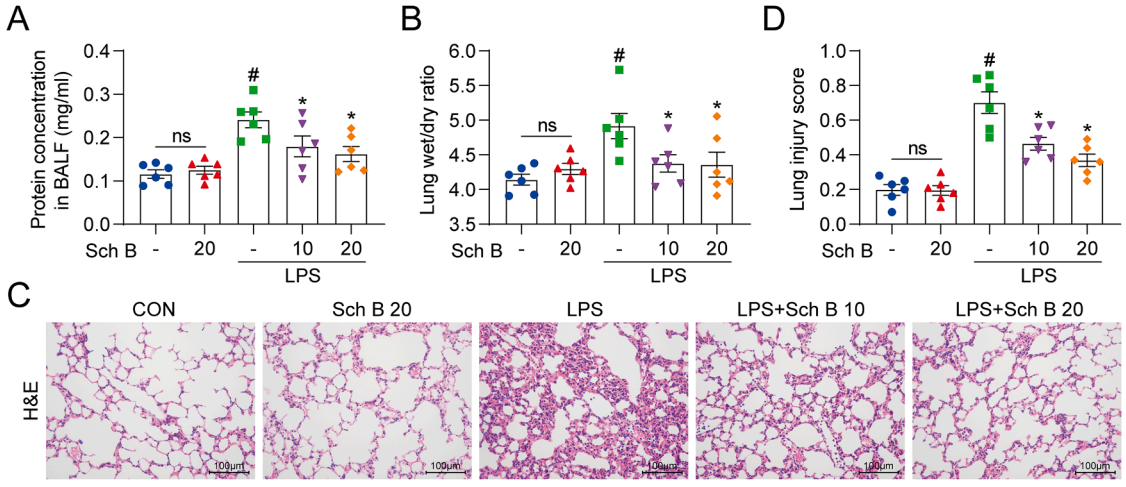

Fig. 4. Sch B suppresses LPS-induced acute lung injury in mice. Mice were challenged with intratracheal LPS (5 mg·kg^{-1}) for 6 h to generate a model of lung injury. The effect of Sch B pretreatment was assessed. (A) Total proteins in BALF samples were measured. (B) Lung wet/dry ratio. (C) Representative H&E stained lung tissues [scale bar = 100 μm]. (D) Quantification of lung injury scores. Data are shown in Mean ± SEM; n=6 *per* group; ns = not significant; # p <0.05 compared to CON; * p <0.05 compared to LPS.

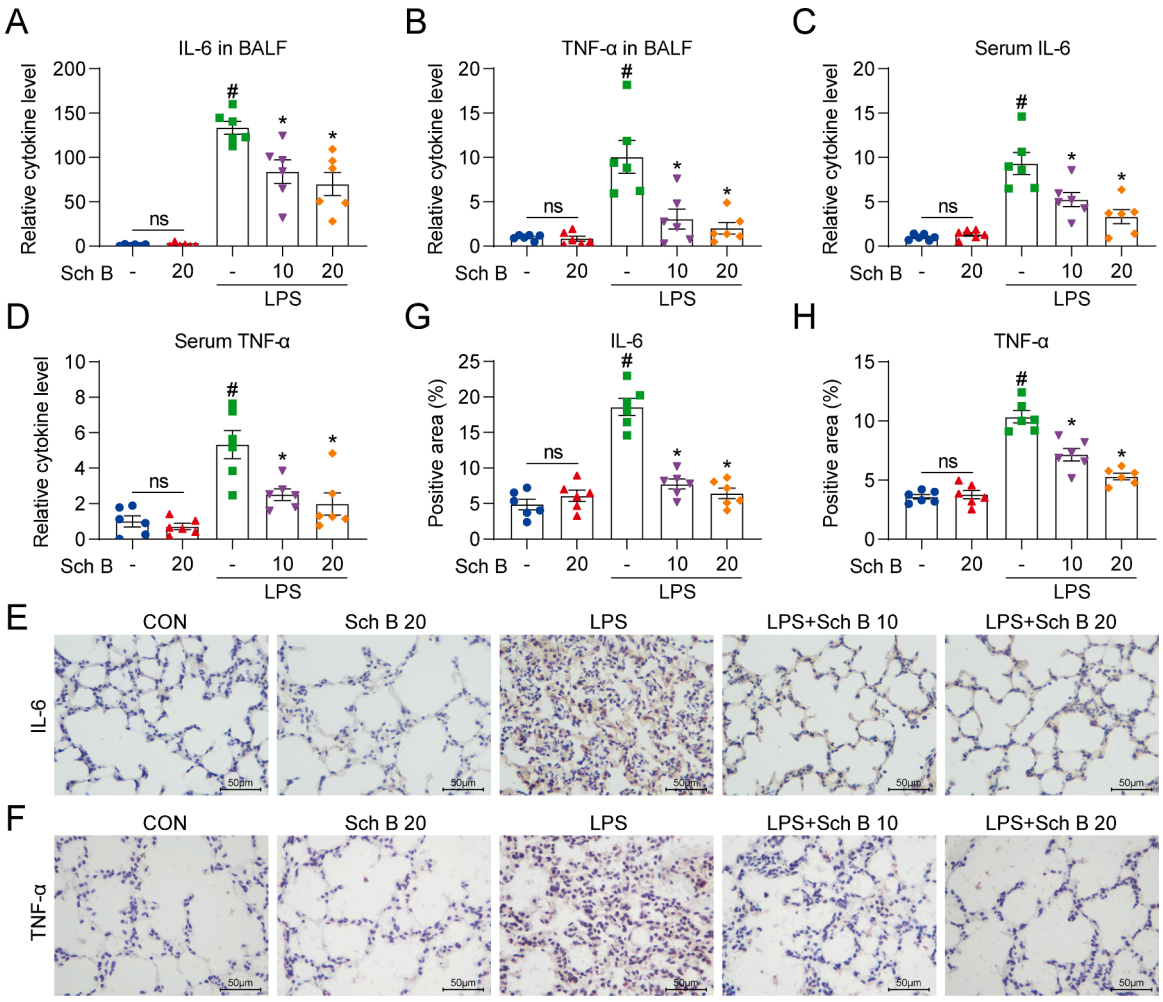

Fig. 5. Sch B reduces LPS-induced circulating and lung inflammatory cytokine levels in mice. (A-D) Levels of IL-6 and TNF-α in BALF samples (A, B) and serum (C, D) in mice challenged with LPS. (E, F) Representative immunostaining of mouse lung tissues for IL-6 and TNF-α. Immunoreactivity was detected by DAB (brown). Slides were counterstained with hematoxylin (blue) [scale bars = 50 μm]. (G, H) Quantification of IL-6 and TNF-α immunoreactivity. Data shown as % stained area. Data are shown in Mean ± SEM; n=6 *per* group; ns = not significant; # p <0.05 compared to CON; * p <0.05 compared to LPS.

heme-containing peroxidase expressed in neutrophils, showed similar results (Fig. 6C). We then assessed monocytes and macrophages in CD45-gated populations in BALF samples. Monocytes were designated as $CD11b^+$ and $Ly6C^+$, whereas macrophages were detected as $CD11b^+$ and $F4/80^+$. We used these markers based on previous studies showing that CD11b (also known as Mac-1) is expressed on monocytes, macrophages, neutrophils, dendritic cells, NK cells and a subset of other inflammatory cells (Gurski and Dittel, 2022). Ly6C monocytes are also considered to be precursors to macrophages during inflammatory conditions. Our results show that LPS increased monocyte and macrophage counts in BALF samples (Fig. 6D, G). These increases were not evident in mice treated with Sch B. Staining of lung tissues for F4/80 macrophage antigen confirmed the reduction of inflammatory macrophages in Sch B-treated mice (Fig. 6H. I).

Lastly, we probed for MyD88-dependent and TRIF-dependent pathway activation in lung lysates. We show that LPS increased the interaction between TLR4 and MD2, MyD88, and TRIF (Fig. 7A, Supplementary Fig. S4A). Among these, only TLR-MyD88 interaction was reduced by Sch B treatment in LPS-challenged mice. Analysis of TAK1, MAPK and IκBα (MyD88-pathway) showed that Sch B suppressed all these LPS-activated pathways (Fig. 7B, Supplementary Fig. S4B). However, no reduction was seen in TBK1 and IRF3 phosphorylation upon Sch B treatment, indicating that TRIF-pathway is not altered by Sch B (Fig. 7C, Supplementary Fig. S4C). mRNA levels of factors downstream of these two TLR4 pathways confirmed that Sch B modulated MyD88-dependent inflammatory responses but not TRIF-mediated interferon responses (Fig. 7D). Collectively, our studies show that Sch B prevents LPS-induced lung injury in mice by reducing inflammatory cell infiltration, and suppression of MyD88 pathway leading to suppressed pro-inflammatory cytokines.

Discussion

Our primary goal in this study was to investigate the mechanisms by which Sch B provides anti-inflammatory responses in LPS-induced ALI model. This was based on a range of studies of Sch B in other systems showing protective effects against conditions that entail oxidative stress and inflammation. Interestingly, in cultured macrophages exposed to LPS, we discovered that Sch B differentially modulated TLR4 signaling pathways to reduce MyD88-dependent pro-inflammatory cytokine production. Further, we found that Sch B directly bound to and inhibited MyD88. This inhibition prevented MyD88 dimerization and its association with TLRs. Consequently, TAK1 and MAPKs/NF-κB activation in MyD88 arm was dampened, and proinflammatory cytokine expression was suppressed. Surprisingly, these responses were achieved independent of any effect of Sch B on the TRIF arm of TLR4 pathway. We validated our findings in the mouse model of LPS-induced ALI. Similar to our results in macrophages, we found that Sch B only inhibited MyD88,

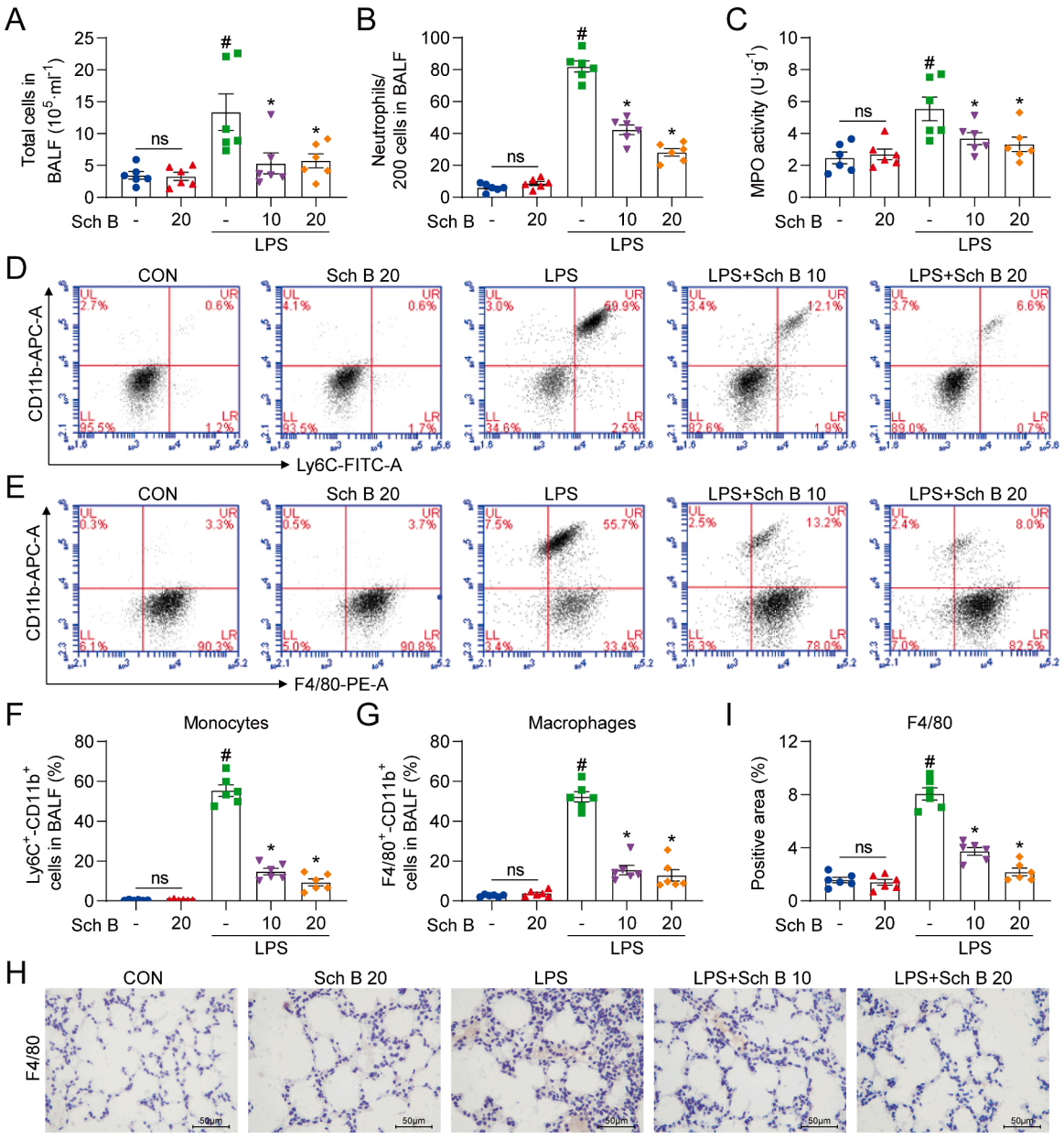

Fig. 6. Sch B reduces LPS-mediated inflammatory infiltration in lungs. (A, B) Total cell counts in BALF samples measured by hemocytometer (A) and neutrophils as assessed by Wright-Giemsa staining (B). (C) MPO activity level in lung lysates. (D-G) Flow cytometric detection of infiltrating cell populations in BALF samples. Representative flow dot plots are shown in panels D and E. CD11b$^+$-Ly6C$^+$ represent monocyte populations and CD11b$^+$-F4/80$^+$ represent monocyte-derived macrophages. Quantification of monocyte and macrophage populations are presented in panels F and G. (H, I) Immunohistochemical staining of lung tissues for F4/80 macrophage marker. Representative stained section is shown in panel H (DAB staining, brown). Quantification of stained area is presented in panel I. Data are shown in Mean ± SEM; n=6 *per* group; ns = not significant; # p <0.05 compared to CON; * p <0.05 compared to LPS.

reduced the activation of TAK1 and MAPKs/NF-κB, and prevented the elaboration of proinflammatory cytokines. At the tissue level, these changes manifested as reduced inflammatory cell infiltration and significantly improved histopathological injury scores. Thus, our studies identified MyD88 as the target of Sch B and show that Sch B is highly effective in reducing ALI in mice.

In ALI/ARDS, inflammation is both an initiating and disease perpetuating factor. Following direct and indirect insults, macrophages, both resident alveolar macrophages and recruited macrophages from the blood, play a key role in the pathogenesis of ALI/ARDS (Lee et al., 2021; Liu et al., 2022a). Macrophages also help to recruit neutrophils that are observed early in lung tissues (Neupane et al., 2020). Infiltrating cells then generate proinflammatory cytokines (Fajgenbaum and June 2020; Lin et al., 2018), worsen disease stage, and correlate with poor outcome in ALI (Meyer et al., 2021). Based on these observations, we investigated the activity of Sch B in macrophages and infiltrating cells in the lungs of mice challenged with LPS. Using these simple, yet elegant models, we show that Sch B interacted directly with MyD88. There is apparently no effect on mechanisms upstream or lateral to MyD88, including the association of MD2 with TLR4 or TLR4-TRIF complex formation. Inhibition of such a hub (MyD88) had an amplified response as can be seen by the suppression of TAK1, MAPK, NF-κB and a large set of inflammatory genes that were downregulated. A multifactorial effect was also documented in the mouse model of ALI, where Sch B reduced infiltration of immune cells, inflammatory factor induction, and improved histological features. Although macrophages are certainly the major cellular target of Sch B, it is possible that other pulmonary cells also benefitted from Sch B treatment. This should be the focus of a future

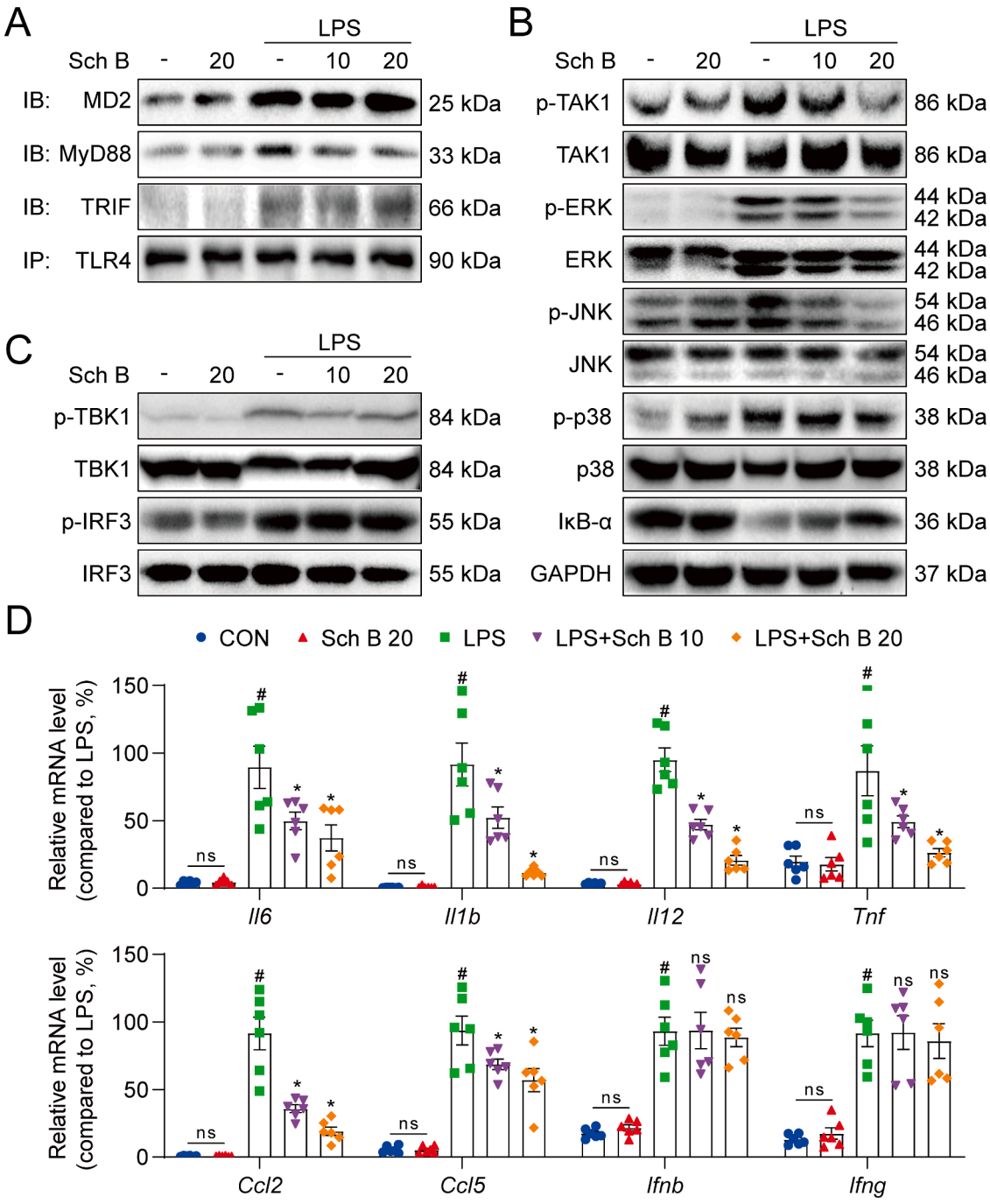

Fig. 7. Sch B treatment is associated with reduced MyD88-dependent pathway proteins, but not TRIF-dependent proteins in lungs. MyD88-dependent and -independent pathway activation was assessed in lung lysates from mice. (A) TLR4 was immunoprecipitated (IP) and levels of MyD88, MD2, and TRIF were detected by immunoblotting (IB). (B, C) Activation of the MyD88-dependent (B) and -independent (C) pathways was assessed by immunoblotting for key proteins in the respective pathways. Unphosphorylated proteins and/or GAPDH were used as control. Representative blots shown. (D) mRNA levels of inflammatory factors in MyD88-dependent and -independent pathway were measured. Data normalized to *Actb*. Data are shown in Mean ± SEM; n=6 *per* group; ns = not significant; # p <0.05 compared to CON; * p <0.05 compared to LPS.

study. In addition, our study did not reveal the SchB-MyD88 interaction at the molecular level. Future experiments are needed to explore the specific binding sites between Sch B and MyD88

Besides, as coronavirus disease 2019 (COVID-19) outbreak all over the world, it is worth noticing that patients infected with COVID-19 start with ALI syndrome (Gallelli et al., 2020; Li et al., 2020). TLR7 and TLR9, which recognize different components of viruses and trigger innate immune responses, have been reported up-regulation after COVID-19 infection and are responsible for the excessive inflammatory response (Luchner et al., 2021; Root-Bernstein, 2021). Coincidentally, both TLR7 and TLR9 are dependent on MyD88 for signaling transduction (Luchner et al., 2021), suggesting the therapeutic potential of Sch B against viruses-induced ALI.

Although our study focused on the discovery of molecular target of Sch B in inhibiting inflammation, it was based on an impressive suite of studies showing antioxidant and anti-inflammatory activity of Sch B. Our group has previously shown that Sch B treatment inhibits NF-κB activity and affords protection against angiotensin II-induced vascular

injury and diabetes-induced nephropathy (Mou et al., 2019; You et al., 2019). Others have reported that Sch B protects against dextran sulfate sodium-induced acute and chronic colitis by suppressing inflammation (Ma et al., 2021). Based on these studies, most others report on an antioxidant role of Sch B. Oxidative stress and inflammation are so intricately linked that it is possibly a given that Sch B also provides antioxidant activity in LPS-induced ALI in mice and in LPS-challenged macrophages. Even though we identified MyD88 as a target, it is likely not the only target of Sch B. We can make this generalization based on our MPO results. Although MPO activity is commonly used as a marker of neutrophils that express MPO robustly (Aratani, 2018), it is also a surrogate marker of oxidative stress. Since Sch B treatment reduced LPS-induced MPO activity in lung lysates, it is likely that this readout also encompasses an antioxidant effect of Sch B. In addition, TLR4/MyD88 inhibition has been reported to reduce ROS level (Hosoi et al., 2021; Wang et al., 2019), suggesting the anti-oxidative effects of Sch B may be partly attributed to targeting MyD88. However, the precise mechanism by which TLR4/MyD88 regulates ROS production is unclear. The experimental evidence would be needed for these conclusions.

A recent study investigated the effect of Sch B in macrophages and concluded that Sch B downregulates the expression of *Myd88* and *Tlr4* (Xu et al., 2018). However, these decreases in expression seen did not correlate with the impressive inhibitory activity of Sch B on NF-κB, as well as MAPK, all measured after a 30-min LPS exposure. The lower mRNA levels of *Tlr4* and *Myd88* are likely capturing the early depression caused by LPS. Studies have shown that in mice, levels of *Tlr4* decrease initially after trans-nasal LPS challenge and start to increase at 4 h, reaching maximal levels at 24 h (Bozinovski et al., 2004; Chang et al., 2021). Our western blot analysis did not reveal significant changes in TLR4 and MyD88 expression levels. However, it should be noted that we performed most of our studies after exposing cells to LPS for 1 or 6 h, which coincides with full TLR4 activation.

One question arising from our study is the functional significance of TRIF-mediated pathway in ALI/ARDS. Signaling through TRIF activates several transcription factors, including IRF3 and AP-1. Such activation may contribute to MyD88 pathway and lead to the production of type-I interferons. It is puzzling that Sch B protected against inflammatory injury in mice and reduced inflammatory factors in cultured macrophages in our study but had no effect on the TRIF pathway. One possible explanation is that TRIF pathway is dispensable, at least, in relation to the major readouts of ALI/ARDS. Studies in support of this notion include the discovery that endotoxin-induced bronchoconstriction, TNF, protein leakage, and neutrophil recruitment in the lung are all abrogated in *Myd88*-deficient mice (Di Padova et al., 2018). Other signals contributing to TLR4 pathways such as TRIF, IL1R and IL18R are found to be dispensable for LPS-induced bronchoconstriction and pulmonary neutrophil sequestration (Di Padova et al., 2018).

Another possibility is that TRIF activation may actually supplement the anti-inflammatory action of Sch B in ALI. A noteworthy thing is that type-I interferons produced *via* TLR4-TRIF activation are very important to activate adaptive immunity. In clinical pathogen-induced sepsis/ALI, an appropriate therapy should avoid to limit the adaptive immunity against pathogens. Studies have shown that TRIF-based agents such as mono-phosphoryl lipid A are used clinically as an adjuvant in cancer, hepatitis, and malaria vaccines and applied in allergen-specific immunotherapy (Wang et al., 2020). These agents display reduced MyD88-dependent signaling activity, but TRIF-dependent signaling activity is similar to the LPS (Hernandez et al., 2016; Watts et al., 2020), possibly conveying immunomodulatory activity. These findings are significant because inhibition of TLR4 with E5564 (Eritoran) and TAK-242 has been tested in humans with severe sepsis/ALI and no significant reduction in 28-day mortality has been shown (Romerio and Peri, 2020). Perhaps targeting MyD88 would be beneficial in suppressing proinflammatory factors while leaving the interferon response intact, which is required for the adaptive immunity against pathogens and likely contributed to the failure of TLR4 therapies against pathogen-induced ALI/ARDS. This interesting avenue (specifically targeting MyD88, rather than the upstream TLR4, to keep TRIF-interferons active) requires further investigation in pathogen-induced models.

Conclusion

In conclusion, this study demonstrates that Sch B exerts anti-inflammatory responses in macrophages and lung tissues challenged by LPS through interacting directly with MyD88. These effects are independent of TRIF activation, as Sch B fails to reduce TLR4-TRIF interaction and induction of interferon response pathway. Our study implicates Sch B as a candidate for drug development and potential use for ALI/ARDS and possibly other MyD88-driven inflammatory diseases. Moreover, further preclinical investigations, such as pathogen-induced models, are required to extend the applications of our findings in the current study.

Supplementary materials

Supplemental information includes Fig. 4 and Table 2. All the data in this study are available upon reasonable request from the corresponding author.

CRediT authorship contribution statement

Weiwei Zhu: Writing – original draft, Investigation. **Wu Luo:** Investigation, Data curation, Formal analysis. **Jibo Han:** Investigation. **Qiuyan Zhang:** Investigation. **Lijun Ji:** Investigation. **Aleksandr V. Samorodov:** Writing – review & editing. **Valentin N. Pavlov:** Writing – review & editing. **Zaishou Zhuang:** Investigation. **Daona Yang:** Investigation. **Lina Yin:** Investigation. **Lijiang Huang:** Writing – review & editing. **Guang Liang:** Conceptualization, Visualization, Data curation, Formal analysis. **Joo Young Huh:** Conceptualization, Visualization. **Yi Wang:** Conceptualization, Visualization, Writing – original draft, Data curation, Formal analysis.

Declaration of Competing Interest

We wish to confirm that there are no known conflicts of interest associated with this publication and there has been no significant financial support for this work that could have influenced its outcome.

Acknowledgments

We thank Dr. Zia Ali Khan (Western Unviersity, Canada) for critical review and editing of the manuscript.

This study was supported by Key Scientific Project of Wenzhou City (ZY2021021 to Y.W.), National Key Research Project (2017YFA0506000 to Y.W.), National Natural Science Foundation of China (21961142009 to G.l., 82000793 to W.l., 82170373 to Y.W., 81770799 to D.Y.), and Zhejiang Provincial Key Scientific Project (2021C03041 to G.l.).

Supplementary materials

Supplementary material associated with this article can be found, in the online version, at doi:10.1016/j.phymed.2022.154489.

References

Aratani, Y., 2018. Myeloperoxidase: its role for host defense, inflammation, and neutrophil function. Arch. Biochem. Biophys. 640, 47–52.

International Natural Product Sciences, T. Atanasov, A.G., Zotchev, S.B., Dirsch, V.M., Supuran, C.T., 2021. Natural products in drug discovery: advances and opportunities Nat. Rev. Drug Discov. 20, 200–216.

Banavasi, H., Nguyen, P., Osman, H., Soubani, A.O., 2021. Management of ARDS - what works and what does not. Am. J. Med. Sci. 362, 13–23.

Bozinovski, S., Jones, J., Beavitt, S.J., Cook, A.D., Hamilton, J.A., Anderson, G.P., 2004. Innate immune responses to LPS in mouse lung are suppressed and reversed by

neutralization of GM-CSF *via* repression of TLR-4. Am. J. Physiol. Lung Cell Mol. Physiol. 286, L877–L885.
Chang, C., Hu, L., Sun, S., Song, Y., Liu, S., Wang, J., Li, P., 2021. Regulatory role of the TLR4/JNK signaling pathway in sepsisinduced myocardial dysfunction. Mol. Med. Rep. 23, 334.
Chen, L., Chen, H., Chen, P., Zhang, W., Wu, C., Sun, C., Luo, W., Zheng, L., Liu, Z., Liang, G., 2019. Development of 2-amino-4-phenylthiazole analogues to disrupt myeloid differentiation factor 88 and prevent inflammatory responses in acute lung injury. Eur. J. Med. Chem. 161, 22–38.
Chen, Y., Kong, Y., Wang, Q., Chen, J., Chen, H., Xie, H., Li, L., 2021. Schisandrin B attenuates airway inflammation by regulating the NF-κB/Nrf2 signaling pathway in mouse models of asthma. J. Immunol. Res. 2021, 8029963.
Ciesielska, A., Matyjek, M., Kwiatkowska, K., 2021. TLR4 and CD14 trafficking and its influence on LPS-induced pro-inflammatory signaling. Cell Mol. Life Sci. 78, 1233–1261.
D'Alessio, F.R., 2018. Mouse models of acute lung injury and ARDS. Methods Mol. Biol. 1809, 341–350.
Di Padova, F., Quesniaux, V.F.J., Ryffel, B., 2018. MyD88 as a therapeutic target for inflammatory lung diseases. Expert Opin. Ther. Targets 22, 401–408.
Dutta, D., Jana, M., Majumder, M., Mondal, S., Roy, A., Pahan, K., 2021. Selective targeting of the TLR2/MyD88/NF-κB pathway reduces α-synuclein spreading *in vitro* and *in vivo*. Nat. Commun. 12, 5382.
Fajgenbaum, D.C., June, C.H., 2020. Cytokine Storm. N. Engl. J. Med. 383, 2255–2273.
Fitzgerald, K.A., Kagan, J.C., 2020. Toll-like receptors and the control of immunity. Cell 180, 1044–1066.
Gallelli, L., Zhang, L., Wang, T., Fu, F., 2020. Severe acute lung injury related to COVID-19 infection: a review and the possible role for Escin. J. Clin. Pharmacol. 60, 815–825.
Gao, Y., Wu, S., Cong, R., Xiao, J., Ma, F., 2019. Characterization of lignans in Schisandra chinensis oil with a single analysis process by UPLC-Q/TOF-MS. Chem. Phys. Lipids 218, 158–167.
Gurski, C.J., Dittel, B.N., 2022. Myeloperoxidase as a marker to differentiate mouse monocyte/macrophage subsets. Int. J. Mol. Sci. 23, 8246.
Hernandez, A., Bohannon, J.K., Luan, L., Fensterheim, B.A., Guo, Y., Patil, N.K., McAdams, C., Wang, J., Sherwood, E.R., 2016. The role of MyD88- and TRIF-dependent signaling in monophosphoryl lipid A-induced expansion and recruitment of innate immunocytes. J. Leukoc. Biol. 100, 1311–1322.
Hosoi, T., Yamawaki, Y., Kimura, H., Honda, S., Ozawa, K., 2021. Possible involvement of MyD88 in regulating stress response in mice. Front. Neurosci. 15, 621446.
Kany, S., Vollrath, J.T., Relja, B., 2019. Cytokines in inflammatory disease. Int. J. Mol. Sci. 20, 6008.
Kopustinskiene, D.M., Bernatoniene, J., 2021. Antioxidant Effects of Schisandra chinensis Fruits and Their Active Constituents. Antioxidants (Basel) 10, 620.
Lee, J.W., Chun, W., Lee, H.J., Min, J.H., Kim, S.M., Seo, J.Y., Ahn, K.S., Oh, S.R., 2021. The role of macrophages in the development of acute and chronic inflammatory lung diseases. Cells 10, 897.
Li, L., Huang, Q., Wang, D.C., Ingbar, D.H., Wang, X., 2020. Acute lung injury in patients with COVID-19 infection. Clin. Transl. Med. 10, 20–27.
Lin, S., Wu, H., Wang, C., Xiao, Z., Xu, F., 2018. Regulatory T cells and acute lung injury: cytokines, uncontrolled inflammation, and therapeutic implications. Front. Immunol. 9, 1545.
Liu, C., Xiao, K., Xie, L., 2022a. Advances in the regulation of macrophage polarization by Mesenchymal stem cells and Implications for ALI/ARDS treatment. Front. Immunol. 13, 928134.
Liu, C., Xiao, K., Xie, L., 2022b. Advances in the use of exosomes for the treatment of ALI/ARDS. Front. Immunol. 13, 971189.
Luchner, M., Reinke, S., Milicic, A., 2021. TLR agonists as vaccine adjuvants targeting cancer and infectious diseases. Pharmaceutics 13, 142.
Ma, Z., Xu, G., Shen, Y., Hu, S., Lin, X., Zhou, J., Zhao, W., Liu, J., Wang, J., Guo, J., 2021. Schisandrin B-mediated TH17 cell differentiation attenuates bowel inflammation. Pharmacol. Res. 166, 105459.
Matthay, M.A., Zemans, R.L., Zimmerman, G.A., Arabi, Y.M., Beitler, J.R., Mercat, A., Herridge, M., Randolph, A.G., Calfee, C.S., 2019. Acute respiratory distress syndrome. Nat. Rev. Dis. Prim. 5, 18.
Meyer, N.J., Gattinoni, L., Calfee, C.S., 2021. Acute respiratory distress syndrome. Lancet 398, 622–637.
Moncrieffe, M.C., Bollschweiler, D., Li, B., Penczek, P.A., Hopkins, L., Bryant, C.E., Klenerman, D., Gay, N.J., 2020. MyD88 death-domain oligomerization determines myddosome architecture: implications for toll-like receptor signaling. Structure 28, 281–289 e283.
Mou, Z., Feng, Z., Xu, Z., Zhuang, F., Zheng, X., Li, X., Qian, J., Liang, G., 2019. Schisandrin B alleviates diabetic nephropathy through suppressing excessive inflammation and oxidative stress. Biochem. Biophys. Res. Commun. 508, 243–249.
Nasser, M.I., Zhu, S., Chen, C., Zhao, M., Huang, H., Zhu, P., 2020. A comprehensive review on Schisandrin B and its biological properties. Oxid. Med. Cell. Longev. 2020, 2172740.
Neupane, A.S., Willson, M., Chojnacki, A.K., Vargas, E.S.C.F., Morehouse, C., Carestia, A., Keller, A.E., Peiseler, M., DiGiandomenico, A., Kelly, M.M., Amrein, M., Jenne, C., Thanabalasuriar, A., Kubes, P., 2020. Patrolling alveolar macrophages conceal bacteria from the immune system to maintain homeostasis. Cell 183, 110–125 e111.
Nowak, A., Zakłos-Szyda, M., Błasiak, J., Nowak, A., Zhang, Z., Zhang, B., 2019. Potential of Schisandra chinensis (Turcz.) Baill. in human health and nutrition: a review of current knowledge and therapeutic perspectives. Nutrients 11, 333.
3rd Paris, A.J., Hayer, K.E., Oved, J.H., Avgousti, D.C., Toulmin, S.A., Zepp, J.A., Zacharias, W.J., Katzen, J.B., Basil, M.C., Kremp, M.M., Slamowitz, A.R., Jayachandran, S., Sivakumar, A., Dai, N., Wang, P., Frank, D.B., Eisenlohr, L.C., Cantu, E., Beers, M.F., Weitzman, M.D., Morrisey, E.E., Worthen, G.S., 2020. STAT3-BDNF-TrkB signalling promotes alveolar epithelial regeneration after lung injury. Nat. Cell Biol. 22, 1197–1210.
Rahman, M.M., Bibi, S., Rahaman, M.S., Rahman, F., Islam, F., Khan, M.S., Hasan, M.M., Parvez, A., Hossain, M.A., Maeesa, S.K., Islam, M.R., Najda, A., Al-Malky, H.S., Mohamed, H.R.H., AlGwaiz, H.I.M., Awaji, A.A., Germoush, M.O., Kensara, O.A., Abdel-Daim, M.M., Saeed, M., Kamal, M.A., 2022. Natural therapeutics and nutraceuticals for lung diseases: traditional significance, phytochemistry, and pharmacology. Biomed. Pharmacother. 150, 113041.
Rao, L.Z., Wang, Y., Zhang, L., Wu, G., Zhang, L., Wang, F.X., Chen, L.M., Sun, F., Jia, S., Zhang, S., Yu, Q., Wei, J.H., Lei, H.R., Yuan, T., Li, J., Huang, X., Cheng, B., Zhao, J., Xu, Y., Mo, B.W., Wang, C.Y., Zhang, H., 2021. IL-24 deficiency protects mice against bleomycin-induced pulmonary fibrosis by repressing IL-4-induced M2 program in macrophages. Cell Death Differ. 28, 1270–1283.
Romerio, A., Peri, F., 2020. Increasing the chemical variety of small-molecule-based TLR4 modulators: an overview. Front. Immunol. 11, 1210.
Root-Bernstein, R., 2021. Innate receptor activation patterns involving TLR and NLR synergisms in COVID-19, ALI/ARDS and sepsis cytokine storms: a review and model making novel predictions and therapeutic suggestions. Int. J. Mol. Sci. 22, 2108.
Rybnikar, M., Smejkal, K., Zemlicka, M., 2019. Schisandra chinensis and its phytotherapeutical applications. Ces. Slov. Farm. 68, 95–118.
Wang, Y., Hu, H., Yin, J., Shi, Y., Tan, J., Zheng, L., Wang, C., Li, X., Xue, M., Liu, J., Wang, Y., Li, Y., Li, X., Liu, F., Liu, Q., Yan, S., 2019. TLR4 participates in sympathetic hyperactivity Post-MI in the PVN by regulating NF-κB pathway and ROS production. Redox Biol. 24, 101186.
Wang, Y.Q., Bazin-Lee, H., Evans, J.T., Casella, C.R., Mitchell, T.C., 2020. MPL adjuvant contains competitive antagonists of human TLR4. Front. Immunol. 11, 577823.
3rd Watts, B.A., Tamayo, E., Sherwood, E.R., Good, D.W., 2020. Monophosphoryl lipid a pretreatment suppresses sepsis- and LPS-induced proinflammatory cytokine production in the medullary thick ascending limb. Am. J. Physiol. Ren. Physiol. 319, F8–F18.
Wong, J.J.M., Leong, J.Y., Lee, J.H., Albani, S., Yeo, J.G., 2019. Insights into the immuno-pathogenesis of acute respiratory distress syndrome. Ann. Transl. Med. 7, 504.
Wu, Y., Li, Z.C., Yao, L.Q., Li, M., Tang, M., 2019. Schisandrin B alleviates acute oxidative stress *via* modulation of the Nrf2/Keap1-mediated antioxidant pathway. Appl. Physiol. Nutr. Metab. 44, 1–6.
Xu, J., Lu, C., Liu, Z., Zhang, P., Guo, H., Wang, T., 2018. Schizandrin B protects LPS-induced sepsis *via* TLR4/NF-κB/MyD88 signaling pathway. Am. J. Transl. Res. 10, 1155–1163.
You, S., Qian, J., Wu, G., Qian, Y., Wang, Z., Chen, T., Wang, J., Huang, W., Liang, G., 2019. Schizandrin B attenuates angiotensin II induced endothelial to mesenchymal transition in vascular endothelium by suppressing NF-κB activation. Phytomedicine 62, 152955.
Zhao, B., Li, G.P., Peng, J.J., Ren, L.H., Lei, L.C., Ye, H.M., Wang, Z.Y., Zhao, S., 2021. Schizandrin B attenuates hypoxia/reoxygenation injury in H9c2 cells by activating the AMPK/Nrf2 signaling pathway. Exp. Ther. Med. 21, 220.